JOURNAL OF GEOPHYSICAL RESEARCH, VOL. 89, NO. C1, PAGES 641–648, JANUARY 20, 1984

Thermohaline Stratification Below the Southern Ocean Sea Ice

ARNOLD L. GORDON AND BRUCE A. HUBER

Lamont-Doherty Geological Observatory

The end of winter stratification within the cold cyclonic trough of the Weddell gyre near 60°S between 5°E and the Greenwich meridian is resolved with the *Mikhail Somov* data set. The temperature maximum of the Weddell Deep Water (WDW) is, for the most part, less than 0.5°C, but warmer cells of WDW are found. These warm WDW cells have temperature, salinity, and oxygen properties similar to the WDW characteristic of the Weddell gyre inflow, which is situated to the southeast of the *Mikhail Somov* study region. The warm WDW cells are accompanied by domes in the pycnocline of 40 m amplitude over the surrounding pycnocline, while deeper isopycnals are depressed. Anticyclonic shear below the 27.83 σ-θ isopycnal within the warm WDW cells is compensated by the cyclonic shear associated with the pycnocline dome. The pycnocline domes are exposed to about 50% greater entrainment by the turbulently active winter mixed layer, relative to the regional entrainment rate. This entrainment can significantly erode the warm cells in a single winter season, introducing excess heat and salt into the mixed layer. While the heat is lost to the atmosphere, the excess salt is not necessarily compensated by increased fresh water introduction. It is hypothesized that the warm WDW cells within the Weddell gyre trough are derived from instability within the frontal zone which extends from Maud Rise to the northeast, separating the Weddell warm regime from the cold regime. Greater than normal injection of warm WDW cells into the Weddell gyre trough would increase the surface salinity, which would tend to destabilize the pycnocline, increasing the probability of deep convection and polynya events.

1. INTRODUCTION

During October and November 1981 the joint U.S.-U.S.S.R. Weddell Polynya Expedition was carried out within the Southern Ocean sea ice, aboard the Soviet ship *Mikhail Somov* of the Arctic-Antarctic Research Institute of Leningrad [*Gordon and Sarukhanyan*, 1982; *Gordon*, 1982]. The objectives of the expedition were to obtain a comprehensive interdisciplinary data set near the Greenwich meridian (0°E), well within the seasonal sea ice zone and to investigate an active open ocean polynya. A polynya developed near 65°S and 0°E in the 1974–1976 winters [*Carsey*, 1980]; however, no polynya developed in 1981. The observations extend across the ice edge zone into the interior pack about 590 km from the mean position of the outer fringes of sea ice during the expedition.

The *Mikhail Somov* hydrographic data set resolves the thermohaline stratification during the transition phase from waxing to waning of the Southern Ocean sea ice cover. Sea ice covers the region near 60°S between 0° and 5°E in June, reaching a maximum northward extent during September and October. The region becomes ice free in mid-December (Antarctic Ice Charts, Navy-NOAA Joint Ice Center, Naval Polar Oceans Center, Suitland, Maryland). In 1981 the ice edge overtook the region between June 18 and 25, remained near 56°S from the end of July to early November, and retreated from the region during the third week of December. The *Mikhail Somov* data set reveals the cumulative effects of the 1981 austral winter and thus depicts the end of winter stratification, although the expedition took place in the austral spring.

The positions of the CTD-O_2/Rosette hydrographic stations and the expendable bathythermograph (XBT) observations [*Huber et al.*, 1983], as well as ice core sites [*Ackley et al.*, 1982] and the ice edge position at the time of entry and exit from the pack ice are given as Figure 1.

2. OCEANOGRAPHIC SETTING

Most of the *Mikhail Somov* hydrographic stations fall within the trough of the cyclonic Weddell gyre [*Deacon*, 1976, 1979; *Gordon et al.*, 1981; *Gordon and Molinelli*, 1982, plates 231–233]. This region is characterized by a relatively cold (less than 0.5°C) Weddell Deep Water (WDW) and is here designated as the Weddell cold regime (Figure 2). The northern stations fall within the eastward flowing limb of the Weddell gyre, with stations 36 and 37 positioned north of the northern boundary of the Weddell gyre. The boundary is marked by a slight increase in baroclinicity and a transition into deep water far too warm (well in excess of 1°C at the temperature maximum; Figure 3) to have participated in the upstream segment of the Weddell gyre. This warmer deep water is called Circumpolar Deep Water (CDW).

South of the *Mikhail Somov* data set, historical (summer) data reveal the westward flowing limb of the Weddell gyre, with warmer WDW (temperature maximum of up to 1.1°C), here designated the Weddell warm regime. The warmer WDW is derived from the main mass of CDW in the vicinity of 20°–30°E [*Deacon*, 1979]. It appears as a wedge of warm WDW with its apex near Maud Rise (Figure 2). A rather abrupt transition to the Weddell cold regime occurs to the west of Maud Rise (Figure 4) and extends to the northeast from Maud Rise. The transition from cold to warm regimes occurs within a distance of 100 km (e.g., between *Islas Orcadas* stations 95 and 96; Figure 5). The increase in WDW temperature of over 0.4°C is accompanied by a decrease in depth of the temperature maximum from 425 m to 240 m and shallowing of the pycnocline by approximately 50 m. An *Islas Orcadas* section along 20°E (Figure 6) shows a similar transition occuring between stations 75 and 76.

Thus, there is a relatively sharp transition from warm to cold regime coinciding with southwest flow within the Weddell gyre (Figure 2). It is marked by the 0.6° to 0.8°C isotherms of the temperature maximum, extending from 58°S 20°E to 63°S 2°E. The historical data set suggests that this is a climatic feature (e.g., see 350 m temperature section plate 23 of *Gordon and Molinelli* [1982]).

The primary advective path of warm WDW into the western hemisphere occurs south of Maud Rise, over the continental slope where a relatively strong westward current exists (Figure 2) [*Tchernia*, 1977; *Foster and Carmack*, 1976]. Outside the boundary currents the Weddell gyre is sluggish with

Paper number 3C1642.
0148-0227/84/003C-1642$05.00

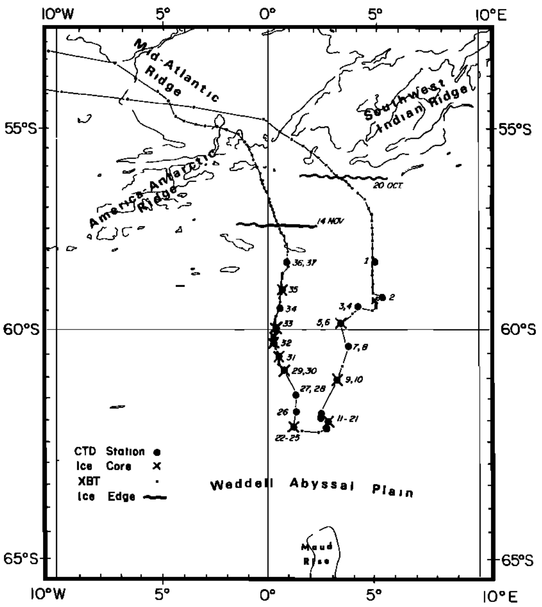

Fig. 1. Cruise track and station sites of the *Mikhail Somov* during the U.S.-U.S.S.R. Weddell Polynya Expedition, October–November 1981.

characteristic velocity of only 1 cm/s [*Gordon et al.*, 1981].

The hydrographic data along the two north-south sections obtained by *Mikhail Somov* (Figures 3 and 7) reveal three structures associated with lateral variations of WDW temperature and pycnocline depth. These structures are (1) the warmer deep water observed at CTD stations 36 and 37 and by the series of expendable bathythermograph (XBT) observations north of the *Mikhail Somov* hydrographic station grid (Figure 8); (2) very cold WDW at station 35; and (3) isolated cells of warm WDW within the Weddell cold regime (above 0.6°C at the temperature maximum).

The warm feature from 57°40′S to 58°40′S on the 0° XBT section (lower panel of Figure 8) is apparently an eddy of CDW. The CDW characteristics within the eddy as revealed at CTD station 36 and 37 extend to 1100 m before yielding to a local oxygen minimum with WDW characteristics [*Huber et al.*, 1983]. The primary transition from Weddell gyre to Circumpolar Deep Water (CDW) occurs near 56°45′S on both XBT sections.

The anomalously cold WDW observed at station 35 (temperature maximum of only 0.19°C at 600 m) and at XBT 103, 109, and 113 surrounds the CDW eddy. This cold deep water is probably an eastward extension of the Weddell-Scotia confluence [*Patterson and Sievers*, 1980].

3. WARM WDW CELLS

The warm WDW cells have not previously been observed within the Weddell cold regime, though the historical data set is too sparse to exclude the possibility of their existence during the summer.

The warm cells are represented in temperature-salinity (θ/S) space (Figure 9) as nearly isohaline extensions above the cold WDW. The WDW of the Weddell warm regime and CDW just north of the Weddell gyre have the same nearly isohaline θ/S form above 0.4°C [*Huber et al.*, 1983; *Gordon and Molinelli*, 1982]. This indicates, as expected, that the source of the warm WDW cells is the deep water surrounding the Weddell cold regime. The warm cells appear within or to the south of a trough in dynamic topography as determined from the *Mikhail Somov* data and have characteristics similar to the WDW of the Weddell warm regime found east of Maud Rise.

The *Mikhail Somov* potential temperature-oxygen (θ/O_2) points (Figure 10) within the warm cells follow the θ/O_2 trend of both the South Atlantic CDW and Weddell warm regime. Oxygen levels within the cells are higher than those within the cold WDW temperature maximum. While it is possible that the warm cells are spawned at the Weddell gyre-CDW front, it is probable that the source is the Weddell warm regime which is closer to the observed warm cells. The warm cells represent a transfer of properties across the transitional zone separating the Weddell cold from the warm deep water regimes.

The other major characteristic of the warm cells is doming of the pycnocline above the cells (Figures 7 and 11). Within the warm cells, where the potential temperature maximum (θ-max) is above 0.5°C, the top of the pycnocline (marked by the depth at which the density increases by more than 0.01 sigma-θ units in 10 m) occurs at an average depth of 74 m. At sites of the cold WDW (θ-max of less than 0.5°C) more typical of the region, the top of the pycnocline occurs at 114 m.

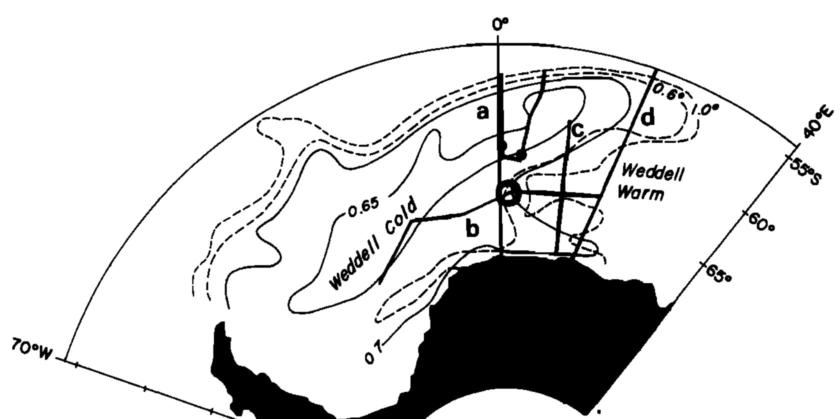

Fig. 2. Schematic of the Weddell gyre. Dashed lines show the isotherms 0.6° and 1.0°C within the oxygen minimum core layer [*Gordon and Molinelli*, 1982, plate 206) which is coincident with the temperature maximum core layer within the Weddell gyre. Solid lines show the 0/2500 dbar isopleths 0.65 and 0.70 dynamic meters [*Gordon and Molinelli*, 1982, plate 230). The *Mikhail Somov* sections (line a) and schematic representation of the warm WDW cells (solid circles) appear north of Maud Rise (large open circle near 65°S and the Greenwich meridian).

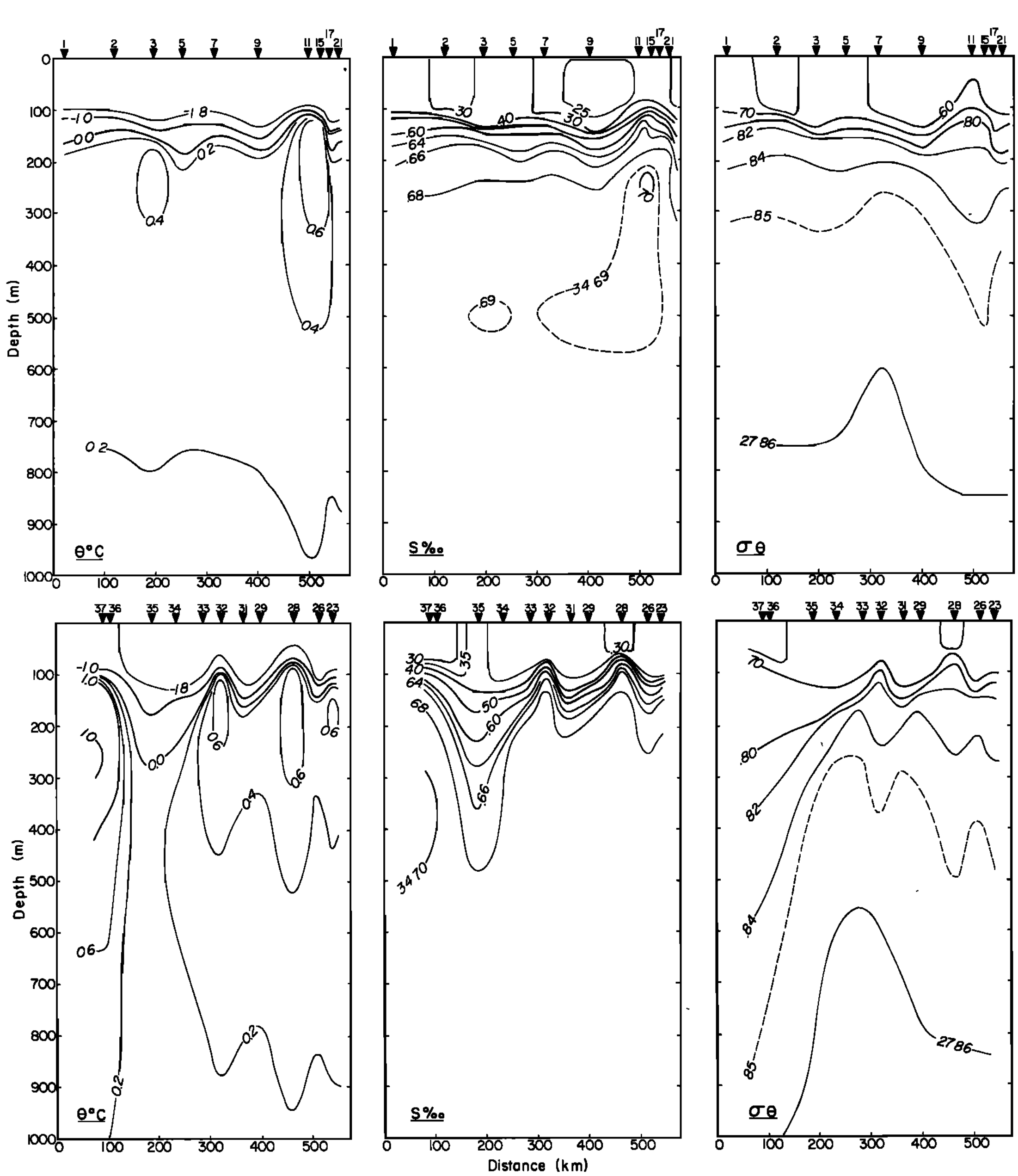

Fig. 3. Potential temperature, salinity, and potential density along the meridional hydrographic sections obtained by *Mikhail Somov* (Figure 1).

Similarly, the depth of the 0°C isotherm increases by about 50 m as the θ-max temperature is reduced from 0.7° to 0.4°C. The same relation is found in the regional *Islas Orcadas* data set.

The warm WDW cells (represented by station 28 and 32) contain an excess of 20.5 Kcal/cm^2 of heat (49 Joules/m^2) and 2.3 gm/cm^2 (23 kg/m^2) of salt relative to the Weddell cold regime water column (represented by stations 31 and 33) above 500 m (Figure 11).

The isopycnal interval 27.82 to 27.83 near 200 m, which coincides with the θ-max, is nearly horizontal, while deeper isopycnals dip below the warm cells (Figure 7). This induces anticyclonic geostrophic shear below 27.83 and cyclonic shear above 27.82. The baroclicity is not great. A maximum geostrophic velocity of only 0.5 cm/s relative to 1900 decibars (dbar) occurs in the 27.82 to 27.83 sigma-θ interval. A secondary velocity maximum of the same magnitude but of opposite sign occurs at the sea surface. The geostrophic velocity at 1900 dbar relative to 5000 dbar (*Mikhail Somov* station pair 29–32) is 0.4 cm/s in the same sense as the θ-max velocity maximum; thus the surface current relative to 5000 dbar is close to zero. Hence, the pycnocline dome effectively compensates the baroclinicity of the rest of the water column. This situation is similar to, though substantially less energetic than, the pycnocline eddies observed in the Arctic [*Newton et al.*, 1974; *Manley*, 1981]. The shear reversal within the upper layer of the Arctic is believed to be induced by secondary Ekman circulation in the ocean boundary layer below the sea ice cover [*Manley*, 1981].

The secondary Ekman circulation associated with the warm WDW cell is extremely weak, inducing a maximum pycnocline upwelling of 10^{-5} to 10^{-6} cm/s. This assumes a circular form of the warm cells, a drag coefficient at the sea ice-water interface of 5×10^{-3} [*Langleben*, 1982; *Andreas*, 1983], and a tangential anticyclonic velocity within the cell of 0.5 to

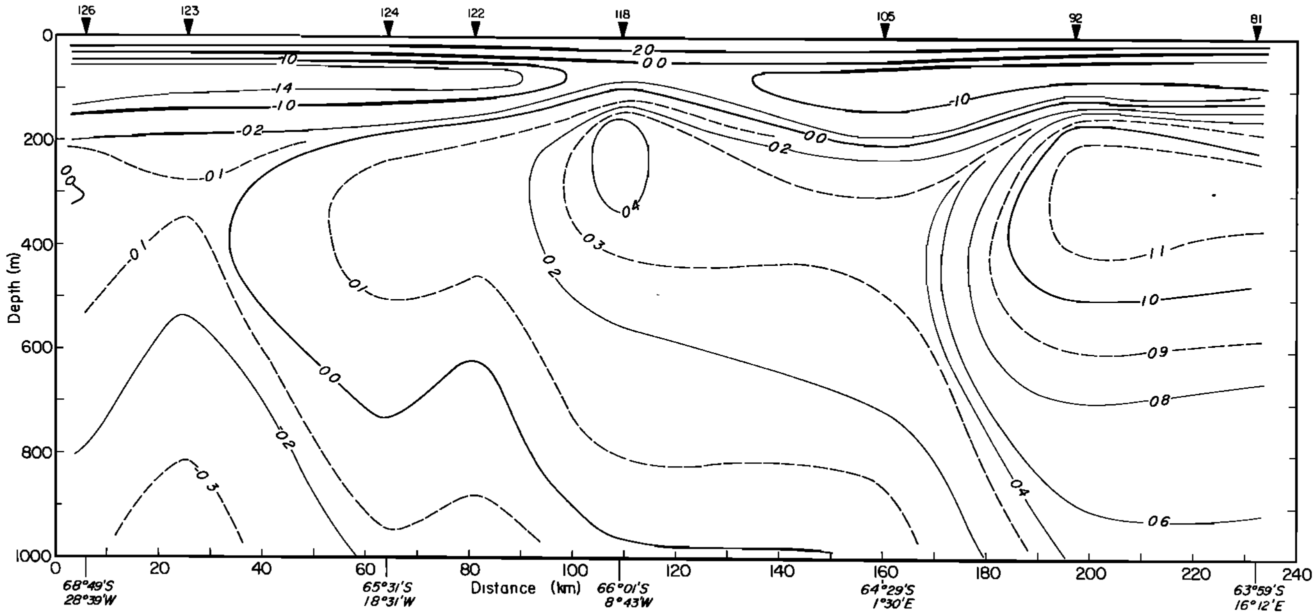

Fig. 4. East-west potential temperature section (line b of Figure 2) from *Islas Orcadas* cruise 12 [*Huber et al.*, 1981].

1.0 cm/s as determined from the geostrophic velocity relative to 1900 and 5000 dbar, respectively. During the ice-covered period this would induce a pycnocline dome of only a meter or two, not the 40 m pycnocline relief observed. It is more likely that the shallow pycnocline associated with a warm WDW cell is a characteristic transferred into the region from the Weddell warm regime.

4. ENTRAINMENT OF THE WARM WDW CELLS

The pycnocline dome of the warm cells is exposed to more intense entrainment by mixed layer turbulence than is the surrounding deeper pycnocline. Within the warm cells the pycnocline intensity is stronger (Figure 11), which may be taken as evidence for enhanced entrainment [*Phillips*, 1977]. *Niiler and Kraus* [1977], in a review of one-dimensional mixed layer models, offer the following equation for mixed layer deepening rate, W_E (cm s^{-1}) in a two layer system:

$$W_E = \frac{2m\ \rho U_*^{\ 3}}{h\ g\Delta\rho} - \frac{n\rho B_0}{g\Delta\rho} \qquad (1)$$

where U_* is the friction velocity defined by $U_* = (C_d U^2)^{1/2}$, ρ is the water density, C_d is the drag coefficient at the ice-water

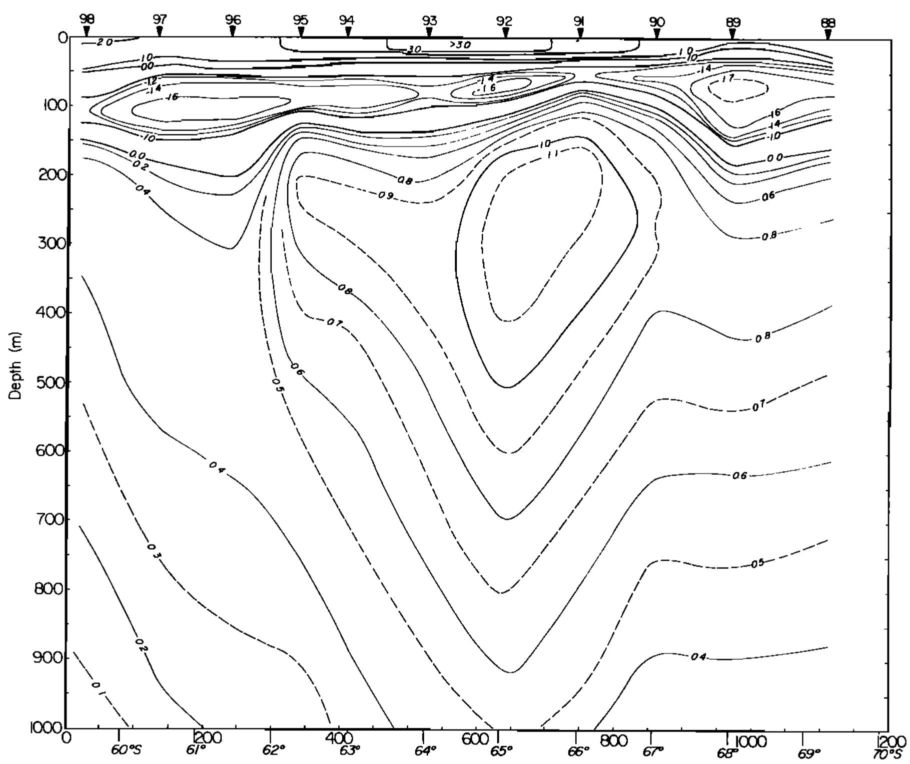

Fig. 5. Potential temperature section along 10°E (line c of Figure 2) from *Islas Orcadas* cruise 12 [*Huber et al.*, 1981].

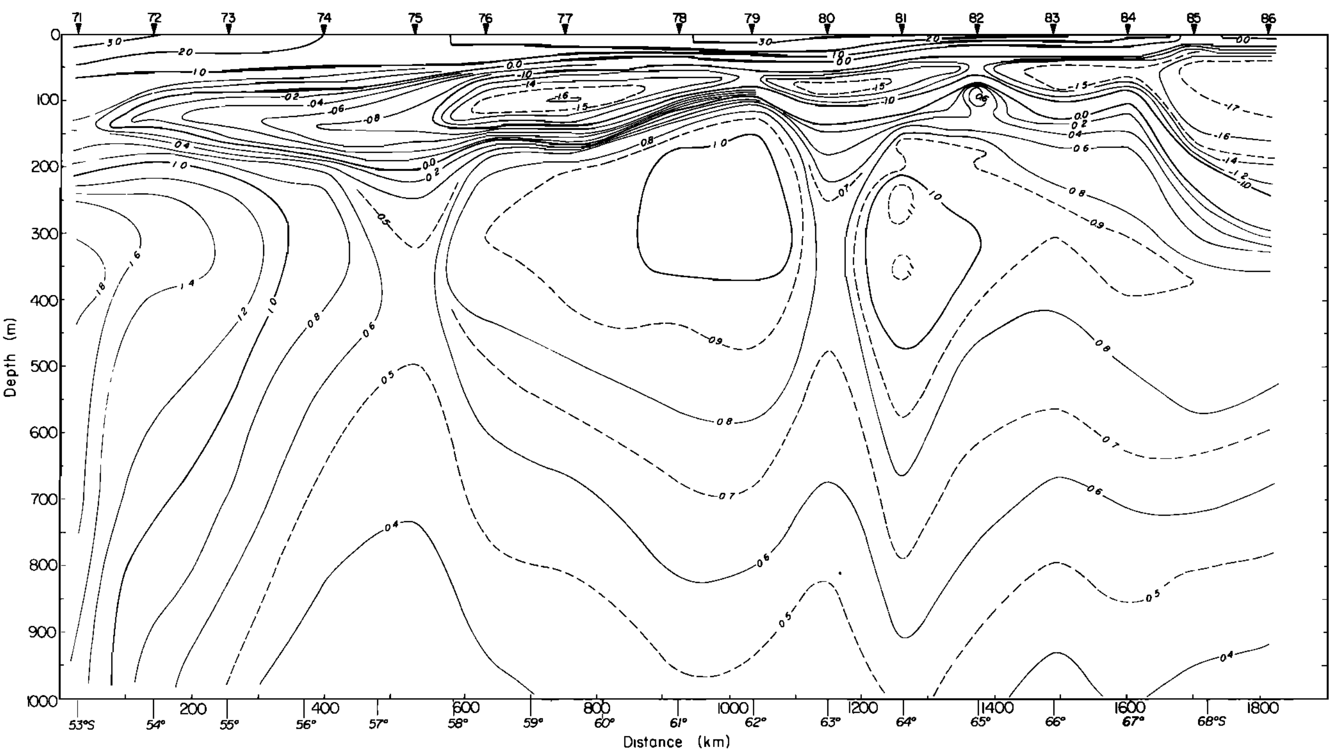

Fig. 6. Potential temperature section along 20°E (line d of Figure 2) from *Islas Orcadas* cruise 12 [*Huber et al.*, 1981].

interface (a value of 5×10^{-3} is used [*Langleben*, 1982; *Andreas*, 1983]); U is the magnitude of the ocean current relative to the ice; h is the mixed layer thickness, taken as 74 m for the warm cells and 114 m for regional value; $\Delta\rho$ is the density difference across the pycnocline, taken as 0.2 σ-θ units; B_0 is the buoyancy flux into the ocean (at the ice-ocean interface $B_0 = g[\beta SF]$ where β is the expansion coefficient for salinity, S is the salinity of the mixed layer, F is the freshwater input to the ocean); g is the acceleration of gravity. The coefficients m and n are proportionality factors. The value of m is taken as 1.25, given by *Kato and Phillips* [1969] though a range of 0.9–2.8 has been suggested [*Cushman-Roisin*, 1981]. The factor n is proportional to the loss of convective energy to dissipation and ranges from 0 to 1 (approaching zero as the mixed layer deepens).

A maximum negative B_0 value would occur if all the observed 75 cm of sea ice [*Ackley et al.*, 1982] were formed locally. Using $n = 0.036$ (*Farmer* [1975] for frozen lakes mixed layer) the entrainment induced by the second term on the right of equation (1) is 2.8×10^{-5} cm s^{-1}. It is likely that much of the sea ice is transported into the region, rather than formed locally (by the end of winter there may be net melting [*Gordon et al.*, 1983]); thus, this represents a maximum value.

From the first term on the right of equation (1) and the relief of the pycnocline over the warm cells the entrainment rate at the pycnocline dome is expected to be 1.54 times larger

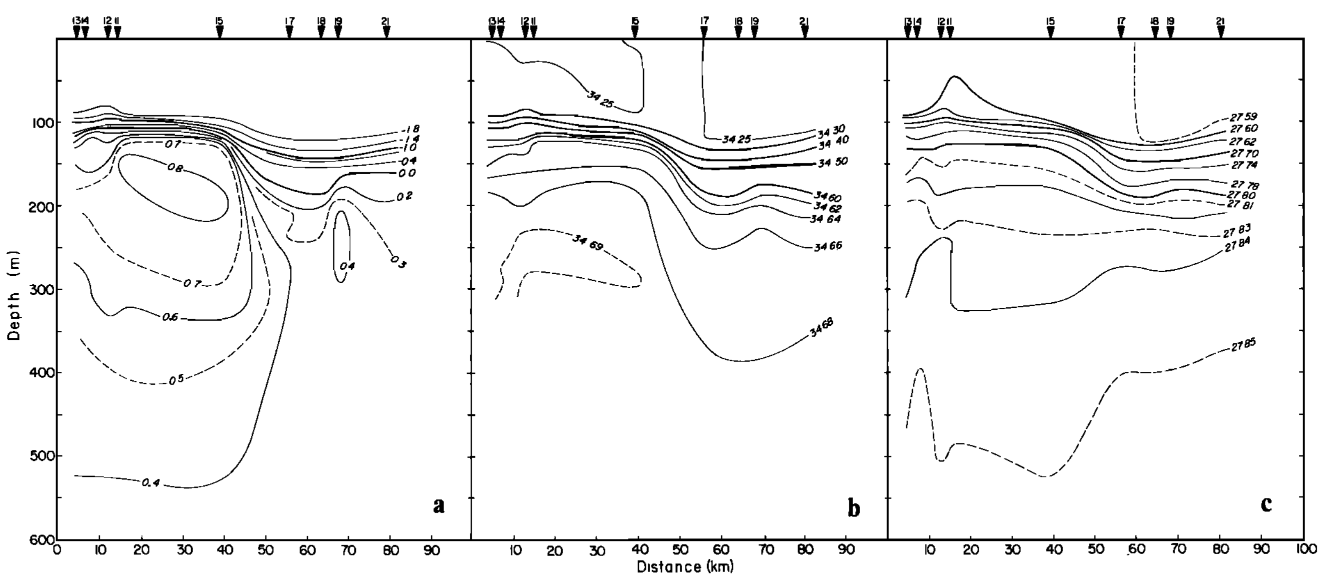

Fig. 7. Expanded scale hydrographic section of the stations within the southeast corner of the *Mikhail Somov* station array (Figure 1).

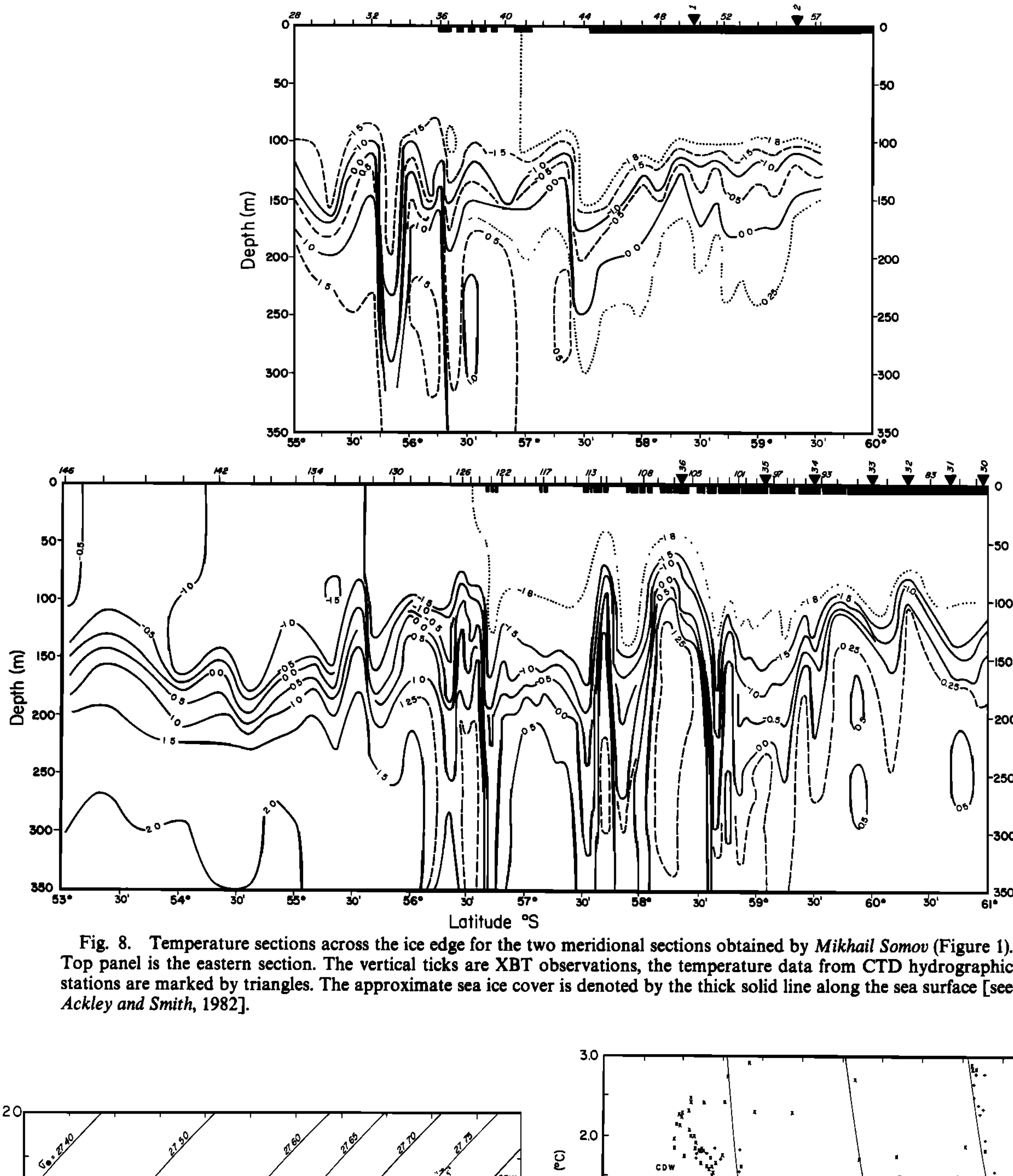

Fig. 8. Temperature sections across the ice edge for the two meridional sections obtained by *Mikhail Somov* (Figure 1). Top panel is the eastern section. The vertical ticks are XBT observations, the temperature data from CTD hydrographic stations are marked by triangles. The approximate sea ice cover is denoted by the thick solid line along the sea surface [see *Ackley and Smith*, 1982].

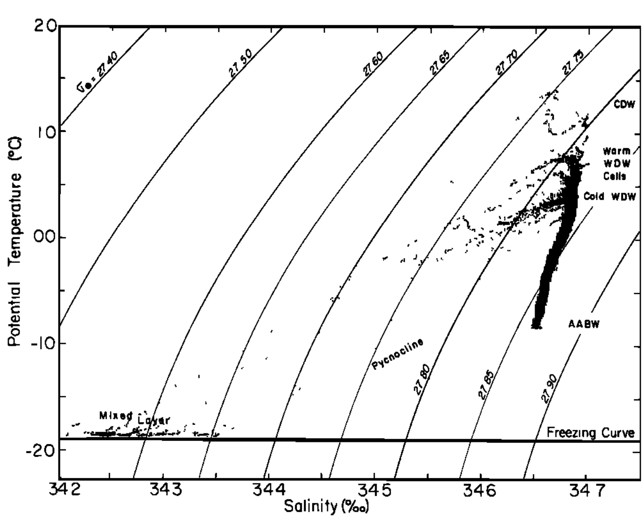

Fig. 9. Potential temperature-salinity relation of the *Mikhail Somov* CTD data.

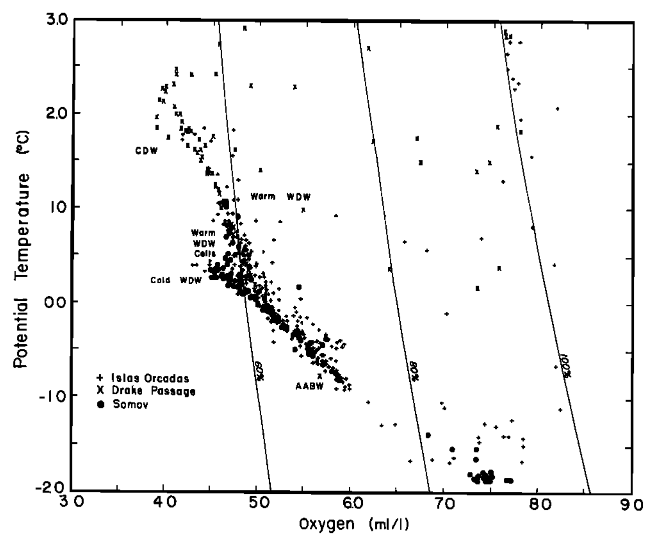

Fig. 10. Potential temperature-oxygen distribution from the *Mikhail Somov* data set, superimposed on select stations from the *Islas Orcadas* cruise 12 and Drake Passage station from FDRAKE-75 data [*Nowlin et al.*, 1977].

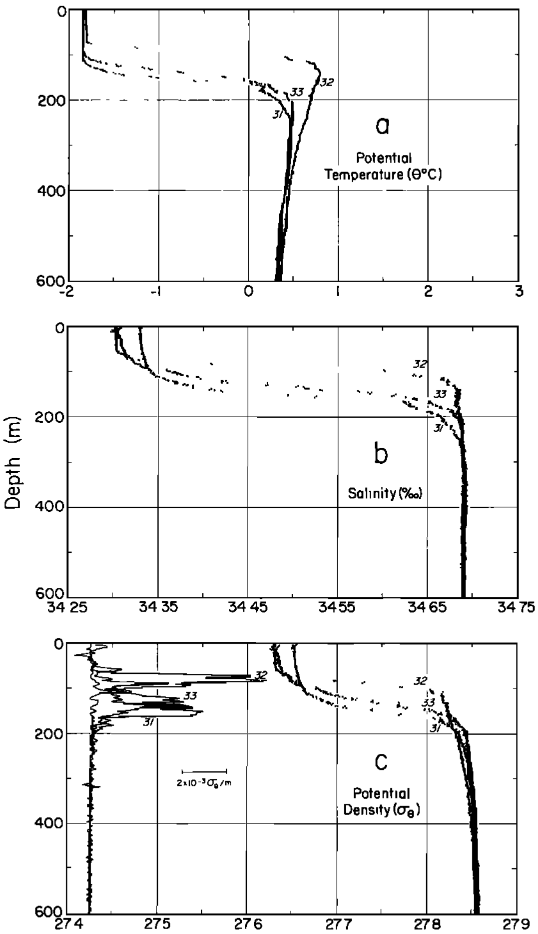

Fig. 11. (*a*) Potential temperature, (*b*) salinity, and (*c*) potential density and vertical gradient of density of three *Mikhail Somov* hydrographic stations across a warm WDW cell (see Figures 1 and 3). The scale bar for density gradient represents a value of 2×10^{-3} σ_θ units per meter.

than the regional rate. Using a value for U of 17 cm/s, based on a 6 hour Soviet current meter record at 60 m [*Huber et al.*, 1983], an estimate of the entrainment rate at the dome is 32.1×10^{-4} cm/s (82 m/month) versus 20.1×10^{-4} cm/s (54 m/month) for the regional deeper pycnocline value.

However, this U value is most likely not representative. In addition, the relative ocean-ice motion at a depth of 1 m, within the logarithmic boundary layer, would be the appropriate value to use with C_d values [*Langleben*, 1982]. Such a value would be significantly less than U at 60 m. For example, calculating U from the winter entrainment rate determined from *Mikhail Somov* oxygen data [*Gordon et al.*, this issue] yields a value of 8 cm/s.

A reasonable conclusion of the entrainment estimates is that the 40 m pycnocline domes of the warm WDW cells would be expected to be significantly attenuated within a single ice-covered season, introducing much of their heat and salt anomaly into the mixed layer. Warm cells that survive the winter would be subject to much less intense entrainment during the summer, when the density difference across the seasonal pycnocline increases to greater than 0.5 σ-θ units.

5. DISCUSSION

As the warm cells are entrained, injecting excess heat and salt into the mixed layer, some impact on mixed layer characteristics is expected. The average mixed layer temperature and salinity observed from *Mikhail Somov* was −1.844°C and 34.287‰, respectively, which is 0.035°C above the freezing point (Figure 9). Pre- and post-cruise calibration of the CTD and independent calibration of the reversing thermometers [*Huber et al.*, 1983] support the significance of the above-freezing mixed layer temperature, which is believed a product of the upward flux of deep water heat. The excess heat would either be lost to the atmosphere in leads and thin ice or be used in the melting of sea ice [*Gordon*, 1981; *Gordon et al.*, this issue]. Presumably, local sea ice production occurs only when the atmosphere removes heat faster than deep water heat is entrained into the mixed layer.

The excess salt introduced to the mixed layer initially may be diluted with sea ice melt, but since all the sea ice melts regionally each spring anyway, the excess salt of the warm WDW cells must ultimately be compensated by an increase in atmospheric water and glacier melt or by net convergence of sea ice. If the salinity anomaly of the warm WDW cells is introduced into the overlying mixed layer within 1 year, then a 67 cm increase in the yearly fresh water input is required locally to produce the mean annual surface water salinity of 34.25‰ [*Gordon et al.*, this issue]. This would more than double the normal annual fresh water input of 45 cm [*Gordon*, 1981].

Naturally, the area over which extra fresh water is required to maintain static stability depends on the degree to which the salinity anomaly spreads laterally within the mixed layer. It may spread rapidly into the entire regional mixed layer, in which case the required extra fresh water demand is not significant, though this ultimately depends on the number of warm cells. It is more likely that the excess salt introduced into the mixed layer is confined to the cell scale of tens of kilometers. Thus the local requirement for fresh water is large and may not be met. In this situation, the warm cell might convert to a convective chimney [*Gordon*, 1978; *Killworth*, 1979]. This interesting possibility deserves further attention.

What relation might the warm WDW cells have to the polynya? The normal route of warm WDW into the Weddell cold regime seems to be by way of a westward flow over the continental slope [*Foster and Carmack*, 1976]. Instability of the frontal zone from Maud Rise to the northeast would inject warm WDW directly into the axial trough of the Weddell cold regime (to the 0.65 dy m isopleth; Figure 2) where it would be advected directly into the deep ocean west of Maud Rise, thus transfering salt into the central region or "hub" of the Weddell gyre. An increase in the transfer of warm WDW cells into the central region of the gyre would increase the salinity of the surface water and decrease the pycnocline stability, unless an increase in fresh water flux accompanies the deep water transfer. This is unlikely since these two processes are not coupled. The decrease of pycnocline stability increases the probability of convective events and the initiation of an open ocean polynya.

What would induce instability and generation of warm WDW cells? An increase in the curl of the wind stress would spin-up the Weddell gyre [*Gordon et al.*, 1981] which would draw more warm saline CDW into the gyre thus increasing the frontal zone intensity between the Weddell warm and cold regimes. Perhaps this would make the front more prone to instability, increasing warm WDW cell generation.

6. CONCLUSION

Instability of the frontal zone separating relatively warm deep water of the Weddell gyre inflow from colder deep water of the Weddell gyre outflow injects WDW cells into cyclonic trough of the Weddell gyre. The excess heat and salt of these cells eventually (of the order of 1 year) enters the surface water. Any increase in the injection rate of these cells, perhaps due to spinup of the Weddell gyre, would force more heat and salt into the central region or hub of the Weddell gyre, which ultimately would enter the surface layer. The excess heat would be lost to the atmosphere, but the excess salt would accumulate unless a commensurate increase in fresh water input occurs, which is unlikely. Thus greater production of warm WDW cells would tend to lower the pycnocline stability making the central region of the Weddell gyre more susceptible to complete pycnocline break down and polynya occurrence.

Acknowledgments. The funding for the U.S.-U.S.S.R. Weddell Polynya Expedition was provided by the Division of Polar Programs of the National Science Foundation. The physical oceanography research is supported by grant DPP 80-05765. Lamont-Doherty Geological Observatory contribution number 3555. Discussions with Hsien Wang Ou were particularly useful. We thank S. S. Jacobs for review of the manuscript.

REFERENCES

Ackley, S. F., and S. J. Smith, Reports of the US-USSR Weddell Polynya Expeditions, Sea Ice Observations, vol. 5, *CRREL Spec. Rep. 83-2*, U.S. Army Corps of Eng., Hanover, N. H., 1983.

Ackley, S. F., D. B. Clarke, and S. J. Smith, Weddell Polynya Expedition preliminary data report: Physical, chemical and biological properties of ice cores, technical note, U.S. Army Cold Regions Res. and Eng. Lab., Hanover, N. H., 1982.

Andreas, E. L., Comment on "Water drag coefficient of first-year sea ice" by M. P. Langleben, *J. Geophys. Res.*, *88*, 779–780, 1983.

Carsey, F. D., Microwave observation of the Weddell Polynya, *Mon. Weather Rev.*, *108*, 2032–2044, 1980.

Cushman-Roisin, B., Deepening of the wind-mixed layer: A model of the vertical structure, *Tellus*, *33*, 564–582, 1981.

Deacon, G. E. R., The cyclonic circulation in the Weddell Sea, *Deep Sea Res.*, *23*, 125–126, 1976.

Deacon, G. E. R., The Weddell Gyre, *Deep Sea Res.*, *26A*, 981–995, 1979.

Farmer, D. M., Penetrative convection in the absence of mean shear, *Q. J. R. Meteorol. Soc.*, *101*, 869–891, 1975.

Foster, T. D., and E. C. Carmack, Temperature and salinty structure in the Weddell Sea, *J. Phys. Oceanogr.*, *6*, 36–44, 1976.

Gordon, A. L., Deep Antarctic convection west of Maud Rise, *J. Phys. Oceanogr.*, *8*, 600–612, 1978.

Gordon, A. L., Seasonality of Southern Ocean sea ice, *J. Geophys. Res.*, *85*, 4193–4197, 1981.

Gordon, A. L., The US-USSR Weddell Polynya Expedition, *Antarctic J.*, *17*, 96–98, 1982.

Gordon, A. L., and E. M. Molinelli, *Southern Ocean Atlas: Thermohaline-Chemical Distributions and the Atlas Data Set*, Columbia University Press, New York, 1982.

Gordon, A. L., and E. I. Sarukhanyan, American and Soviet Expedition into the Southern Ocean sea ice in October and November 1981, *Eos Trans. AGU*, *63*, 2, 1982.

Gordon, A. L., D. G. Martinson, and H. W. Taylor, The wind-driven circulation in the Weddell-Enderby Basin, *Deep Sea Res.*, *28A*, 151–163, 1981.

Gordon, A. L., C. T. A. Chen, and W. G. Metcalf, Winter mixed layer entrainment of Weddell Deep Water, *J. Geophys. Res.*, this issue.

Huber, B., S. Rennie, D. Georgi, S. Jacobs, and A. Gordon, *Ara Islas Orcadas* Data Report, Cruise 12, *Ref. CU-2-81-TR2*, Lamont-Doherty Geol. Observ., Palisades, New York, 1981.

Huber, B. A., J. Jennings, C.-T. Chen, J. Marra, S. Rennie, P. Mele, and A. Gordon, Reports of the US-USSR Weddell Polynya Expedition, Hydrographic data, vol. 2, *L-DGO-83-1*, Lamont-Doherty Geol. Observ., Palisades, New York, 1983.

Kato, H., and O. M. Phillips, On the penetration of a turbulent layer into stratified fluid, *J. Fluid Mech.*, *37*, 643–655, 1969.

Killworth, P. D., On "chimney" formations in the ocean, *J. Phys. Oceanogr.*, *9*, 531–554, 1979.

Langleben, M. P., Water drag coefficient of first-year sea ice, *J. Geophys. Res.*, *87*, 573–578, 1982.

Manley, T. O., Eddies of the western Arctic Ocean: Their characteristics and importance to the energy, heat and salt balance, *CU-1-81, Tech. Rep. 1*, Lamont-Doherty Geol. Obs., Palisades, New York, 1981.

Newton, J. L., K. Aagaard, and L. K. Coachman, Baroclinic eddies in the Arctic Ocean, *Deep Sea Res.*, *21*, 707–719, 1974.

Niiler, P. P., and E. B. Kraus, One-dimensional models of the upper ocean, in *Modelling and Prediction of the Upper Layers of the Ocean*, edited by E. B. Kraus, pp. 143–172, Pergamon, New York, 1977.

Nowlin, W. D. Jr., T. Whitworth III, L. I. Gordon, and G. C. Anderson, Oceanographic station data collected aboard R/V *Melville* during FDRAKE 75, *Ref. 77-2-D*, Texas A&M Res. Foundation, College Station, 1977.

Patterson, S. L., and H. A. Sievers, The Weddell-Scotia confluence, *J. Phys. Oceanogr.*, *10*, 1584–1610, 1980.

Phillips, O. M., Entrainment in *Modelling and Prediction of the Upper Layers of the Ocean*, edited by E. B. Kraus, pp. 92–101, Pergamon, New York, 1977.

Tchernia, P., Etude de la Derive Antarctique Est-Ouest au Moyen d'Ice-bergs Suivio par le Satellite Eole, in *Polar Oceans*, edited by M. J. Dunbar, Arctic Institute of North America, Montreal, Quebec, 1977.

A. L. Gordon and B. A. Huber, Lamont-Doherty Geological Observatory, Columbia University, Palisades, NY 10964.

(Received April 28, 1983;
revised October 6, 1983;
accepted October 6, 1983.)